

A geometric morphometric protocol to correct postmortem body arching in fossil fishes

Carla San Román ^{Corresp., 1, 2}, Hugo Martín-Abad ^{1, 2}, Jesús Marugán-Lobón ^{1, 2}

¹ Unidad de Paleontología, Departamento de Biología, Universidad Autónoma de Madrid, Madrid, Spain

² Centro para la Integración en Paleobiología (CIPb-UAM), Madrid, Spain

Corresponding Author: Carla San Román
Email address: carla.sanroman@uam.es

Postmortem body curvature introduces error in fish morphometric data. Compared to living fish, the causes of such body curvature in fossils may be due to additive taphonomic processes that have been widely studied. However, a protocol that helps to correct its effect upon morphometric data remains unexplored. Here, we test two different mathematical approaches (multivariate regression and the so-called ‘unbending functions’) available to tackle fish geometric morphometric data in two exceptionally preserved gonorynchiformes fossil fishes, *Rubiesichthys gregalis* and *Gordichthys conquensis*, from the Las Hoyas deposits (Early Cretaceous, Spain). Although both methods successfully correct body curvature (i.e., removing misleading geometric variation), our results show that traditional approaches applied in living fishes might not be appropriate to fossil ones, because of the additional anatomical alterations. Namely, the best result for 2D fossil fishes is achieved by correcting the arching of the specimens (mathematically “unbending” them). Ultimately, the effect of body curvature on morphometric data is largely taxon independent and morphological diversity mitigates its effect, but size is an important factor to take into account (because larger individuals tend to be less curved).

1 A geometric morphometric protocol to correct 2 postmortem body arching in fossil fishes.

3

4 Carla San Román^{1,2}, Hugo Martín-Abad^{1,2}, Jesús Marugán-Lobón^{1,2}

5

6 ¹ Unidad de Paleontología, Departamento de Biología, Universidad Autónoma de Madrid,
7 Madrid, Spain8 ² Centro para la Integración en Paleobiología (CIPb-UAM), Madrid, Spain

9

10 Corresponding Author:

11 Carla San Román^{1,2}

12 C/ Darwin, 2, Madrid, 28049, Spain

13 Email address: carla.sanroman@uam.es

14

15 Abstract (500)

16 Postmortem body curvature introduces error in fish morphometric data. Compared to living fish,
17 the causes of such body curvature in fossils may be due to additive taphonomic processes that
18 have been widely studied. However, a protocol that helps to correct its effect upon morphometric
19 data remains unexplored. Here, we test two different mathematical approaches (multivariate
20 regression and the so-called ‘unbending functions’) available to tackle fish geometric
21 morphometric data in two exceptionally preserved gonorynchiformes fossil fishes, *Rubiesichthys*
22 *gregalis* and *Gordichthys conquensis*, from the Las Hoyas deposits (Early Cretaceous, Spain).
23 Although both methods successfully correct body curvature (i.e., removing misleading geometric
24 variation), our results show that traditional approaches applied in living fishes might not be
25 appropriate to fossil ones, because of the additional anatomical alterations. Namely, the best
26 result for 2D fossil fishes is achieved by correcting the arching of the specimens (mathematically
27 “unbending” them). Ultimately, the effect of body curvature on morphometric data is largely
28 taxon independent and morphological diversity mitigates its effect, but size is an important factor
29 to take into account (because larger individuals tend to be less curved).

30

31 Introduction

32 Body arching is a source of non-biological deformation that biases comparative settings,
33 especially those encompassing morphometrics approaches (e.g., Clarke & Friedman, 2018),
34 because it leads to underestimating standard measurements of fish size (i.e., body length).
35 Although it can often be easily solved by applying basic mathematical corrections (e.g., Pan et
36 al., 2019), the problem is strongly accentuated when applying more powerful multidimensional
37 methods of shape analysis such as Geometric Morphometrics, requiring a non-trivial solution
38 (Fruciano et al., 2020; Sotola et al., 2019).

39 The most common method for assessing how to unbend body curvature in living fishes involved
40 gradually arching an individual for taking photographs at selected degrees of body arching
41 (Valentin et al., 2008). The different levels of forced curvature were thereafter assessed as shape
42 changes via landmark data, resulting in a single dominant vector utilized for Burnaby's
43 projection (Burnaby, 1966). Logically, this process is not applicable in fossil fishes, challenging
44 the attainment of a vector that uniquely represents changes in curvature. Furthermore, Burnaby's
45 method for correcting curvature is based on selecting the first dimension of a PCA (PC1) as the
46 expected unique source of curvature. In other words, the method assumes that if curvature is the
47 major source of variation, it will accumulate only in one dimension. However, body arching in
48 fossil fishes alters the variance-covariance matrix, spreading randomly across PCs (i.e., the effect
49 of curvature on the superimposed data becomes latent across multiple dimensions).

50

51 When using landmark data, an alternative method to avoid the effect of body arching is the
52 "Unbending specimens" function implemented in the TpsUtil program (Rohlf, 2008). This
53 function fits a curve along a selection of landmarks that represent the body arching of an
54 individual. The curvature delimited by such landmark configuration is projected onto a straight
55 line according to a quadratic or cubic fit. The rest of landmarks are thereafter translated
56 proportionally until the selected line becomes horizontally straight, representing a landmark
57 configuration of a "straightened fish".

58

59 These mathematical methods available to correct the effect of body-curvature upon Geometric
60 Morphometrics (Procrustes) shape data have only been tested in living fishes (Valentin et al.
61 2008; Haas & Orleans, 2011), but may not work in fossil fishes. This is because many fossil
62 fishes exhibit a wide range of body arching in varying degrees of upward or downward curvature
63 (Bieńkowska-Wasiluk, 2004; Martín-Abad & Poyato-Ariza, 2016a; Cardoso et al., 2020;
64 Chellouche, 2016; Dietl & Schweigert 2011, Hellawell & Orr, 2012; Marramà et al., 2016; San
65 Román et al., 2023; Weiler, 1929). This variety of body arching occurs under uncertain
66 conditions that seem to be related to *rigor mortis*, a process that occurs when fish die and the
67 decay of soft tissue leads to the contraction of muscles and/or ligaments, shortening and bending
68 the backbone (Seilacher et al., 1985; Ando et al., 1990; Roth et al., 2006; Chellouche et al, 2012;
69 Pan et al., 2015; Viohl et al., 2015; Marramà et al., 2016; Martín-Abad & Poyato-Ariza, 2016b).

70

71 Here, we adapt and test the different tools available to mathematically remove the effect of body
72 arching on Geometric Morphometric data in a selected sample of exceptionally well-preserved
73 fossil teleostean species *Rubiesichthys gregalis* and *Gordichthys conquensis*. To such end, we
74 applied the methods to correct curvature without introducing any additional geometric
75 morphometric distortion and tested the correlation with independent data such as body size
76 (allometry).

77

78 **Materials & Methods**

79 We selected 96 individuals, that were complete, fully articulated and preserved in lateral view
80 that belong to the species *Rubiesichthys gregalis* (N=63) and *Gordichthys conquensis* (N=31)
81 from the Las Hoyas fossil site (Early Cretaceous) housed at the Museo Paleontológico of
82 Castilla-La Mancha (MUPA). These two species of gonorynchiform fishes are easily
83 distinguished from each other by a higher body, and shorter and fewer vertebrae in *G.*
84 *conquensis* compared to *R. gregalis* (Fig. 1A, B), among other anatomical features (Poyato-
85 Ariza, 1996).

86 The sample encompasses scale-calibrated pictures using a Canon SX510HS camera on a steady
87 orthogonal position. A configuration of $p=15$ landmarks were evenly placed across the whole
88 fish skeletons using TpsDig2 (Rohlf, 2015), outlining the geometry of the cranium, the body and
89 the relative position of the fins (Fig. 1C, Supplementary File 3: Table 1). To avoid interobserver
90 error, all landmarks were placed by the same person, and to reduce intraobserver error, the
91 process of setting landmarks was repeated three times, and finally the mean landmark
92 configuration was used.

93 The landmark configurations were transformed to shape data using Generalized Procrustes
94 Analysis (Bookstein, 1997), with the packages *geomorph* and *Morpho* (Adams & Otárola-
95 Castillo, 2013; Schlager, 2017) in the R software (v. 4.3.2, R Core Team, 2023).

96

97 Simply repeating the experiment developed by Valentin et al., (2008) of gradually arching an
98 individual is obviously not valid for extracting a vector that uniquely constitutes curvature in
99 fossil fishes. Interestingly, this forced experiment is naturally mimicked by the range of body
100 arching in fossil fishes, which has been traditionally assessed utilizing an index (Index of
101 Curvature, IC; Martín-Abad & Poyato-Ariza, 2016b), that is the ratio between the length from
102 the tip of the snout to the posteriormost end of the hypurals (i.e., the standard length) measured
103 following the curvature of the vertebral column, and the measured in a straight line. Given that
104 we are performing a landmark-based study, we calculated these measurements considering the
105 interlandmark distances resulting from the sum of the distances between landmarks 12, 15, 16,
106 17, 18, 19, and 4, divided by the interlandmark distance between 4 and 12 (Fig. 1D), on the
107 Procrustes standardized data (Fig. 1D). The index varies between 0 and 1 (or alternatively 0-
108 100%), where zero indicates no signal of curvature (body is straight) and one indicates
109 theoretical maximum curvature.

110

111 To explore the relation between the index of curvature and the Procrustes shape data we used a
112 multivariate regression, in order to graphically summarize the values of the index as their
113 corresponding values of shape arching. A Principal Component Analysis (PCA) was used to
114 explore morphological variation in the sample, and linear regression models of each Principal
115 Component (PC) against the index of curvature were performed to test the degree at which body
116 arching could be associated (i.e., randomly disseminated) across PCs (significance level= 0.05).
117 A linear regression model of the index of curvature against the centroid size (the scalar that
118 measures the size of each landmark configuration fossil—i.e., the size of each fish—that is

119 calculated as the square root of the sum of the squared distances between the landmarks;
120 Bookstein, 1997) was used to test the effect of allometry and body arching. We performed
121 Welch's test to assess statistical differences in the curvature between species (i.e., between *R.*
122 *gregalis* and *G. conquensis*).

123

124 The first unbending method that we applied utilizes multivariate regression to remove non-
125 desired measurements from Procrustes data (see e.g., Monteiro et al., 1999; Bräger et al. 2017;
126 Navalón et al., 2022). Accordingly, we applied a multivariate regression of the Procrustes Data
127 against the index of curvature (Monteiro, 1999), using the *procD.lm* function of *geomorph*
128 package (Adams & Otárola-Castillo, 2013). The residuals of such regression are devoid of the
129 effect of index of curvature, by definition, and their transformation back into shape data can be
130 used in subsequent analyses (see details of R coding in Supplementary Data). We termed this
131 first approach "Regression-unbending method".

132

133 As a second approach, we used the "unbending function" of the Tps series (Rohlf, 2015). This
134 function models a curve based on a chosen set of landmarks that depict the curvature of an
135 individual. To such end, we used landmarks 12, 4, four additionally semilandmarks (16-19)
136 placed along the vertebral column (delimited between landmarks 4 and 15), and landmark 15
137 (Fig. 1C,D). The unbending process adjusts the positions of the remaining landmarks in such a
138 way that they maintain their relative proportions while aligning the selected line to be
139 horizontally straight. To maximize the accuracy of the unbending process, the sample was
140 subdivided in seven groups according to their IC scores, ending up in seven partitions. After the
141 unbending process, we removed the semilandmarks that defined the curvature (semilandmarks
142 16-19). Finally, this new shape data was submitted again to a Generalized Procrustes Analysis.
143 We denote this protocol as "Tps-unbending method".

144 The removed effect of body arching is visualized as shape variation across the first six PCs of the
145 Procrustes data for the Regression-unbending and Tps-unbending methods. We calculated the
146 Procrustes variance—squared Euclidean distances between shapes relative to the mean sample
147 shape (Zelditch et al., 2012)—in the total sample and per landmark, for the original and
148 modified data. A pairwise contrast was devised to test differences in the total Procrustes variance
149 of the original versus Regression-unbending data, and the original versus Tps-unbending data.
150 All data management and statistical analyses (except for the "unbending specimens" function
151 performed in TpsUtil) were conducted in R software (v.4.3.2, Team, 2023). The detailed custom-
152 code is available in Supplementary Data.

153

154 Results

155 The original sample shows a mean reduction of 1.37% (IC=0.0137) in standard length due to
156 body arching, with the most curved specimen exhibiting a 6.43% reduction (IC=0.0643) in
157 length (Supplementary File 1, Table 2). Despite this low length reduction, the multivariate
158 regression of the Procrustes Data to the IC shows that IC is associated with shape variance across

159 the whole sample of the Las Hoyas' gonorynchiform fishes (Fig. 2A, $F=20.26$, $df=93$, $p\text{-value}=$
160 0.01 , Supplementary File 3: Table 3). Importantly, results of the PCA clearly show that body
161 arching is not accumulated in a single dimension, as demonstrated by the associations of PC2
162 and PC5 with the IC (Supplementary File 3: Table 4). The linear regression of the IC against the
163 centroid size shows a significant correlation ($F=14.87$, $df=92$, $p\text{-value}<0.01$, Supplementary File
164 3: Table 5), the smallest specimens being the most curved (Fig. 2B). The two studied species,
165 *Rubiesichthys gregalis* and *Gordichthys conquensis*, show similar degrees of body arching
166 ($t=0.48$, $df=57$, $p\text{-value}= 0.951$, Supplementary File 3: Table 6).
167 The PCA of the modified data for the Regression-unbending method seems to capture the
168 presence of shape variation related to body arching in PC1, PC2 and PC4 (Fig. 3), which is also
169 correlated with other aspects of morphology (e.g., body height in PC1, relative size of the
170 cranium and position of dorsal and pectoral fins in PC2). In contrast, the Tps-unbending method
171 indicates absence of shape variation related to body arching in the principal PCs (Fig. 3).
172 The pairwise test comparing original and modified data reveals significant differences in the total
173 Procrustes variances between original and Regression-unbending data, as well as between
174 original and Tps-unbending data. In both cases, the modified data show lower total Procrustes
175 variance than the original data (Supplementary File 3: Table 7-9).
176 Both the Regression-unbending and Tps-unbending methods' data show lower relative
177 Procrustes variances in the extreme of the body (LM 15 and 4, Fig. 4; Supplementary File 3:
178 Table 9) compared to the original data. The highest Procrustes variances are located in LM 1, 2
179 and 8 in the original and in the modified data, accounting for body height (main difference
180 between species).

181

182 Discussion

183 Post-mortem body arching by *rigor mortis* is a common process observed in fishes, that is
184 perfectly visible in the fossil record, and it introduces important biases for statistical inference in
185 morphometric data, particularly when this information is multidimensional (e.g., landmark data).
186 Our results on two well-known gonorynchiform fishes from Las Hoyas, *Rubiesichthys gregalis*
187 and *Gordichthys conquensis*, show that body arching clearly affects morphological variation in
188 different degrees, even when the curvature turned out not to be so pronounced. However, we
189 found that body arching permeates across many dimensions of shape variation, compromising
190 any type of multivariate method that aims at assessing biological processes based on statistical
191 inference (i.e., allometry, modularity). Thus, methods such as Burnaby's, which are expected to
192 correct body arching assuming that it accumulates in a single (dominant) dimension (Valentin et
193 al., 2008), can be ineffective in fossil fishes.

194

195 In the present study, we tested two methods for unbending fossil fishes, namely the Regression-
196 unbending method and the Tps-unbending method. Both methods showed a clear component that
197 dominates the variance and a significant decrease in the Procrustes variance in the modified data
198 compared to the original. However, the Tps-unbending method outperforms the Regression-

199 unbending method in effectively removing the curvature in fossil fishes. Namely, in the
200 Regression-unbending method some remnants of curvature can be detected in the PCs, most
201 likely because details of the body arching are distributed in the variance-covariance matrix and
202 covary with allometry, thus probably comprising subsequent multidimensional analyses. The
203 index of curvature (IC) is too simple to be able to capture the wide range of curvature in fossil
204 fishes (Bieńkowska-Wasiluk et al. 2004, San Román et al., 2023). When utilizing the Tps-
205 unbending method (Haas & Orleans, 2011), on the other hand, the curvature adjusts better to a
206 cubic curve than a quadratic fit, probably because the arching of the bodies is not uniquely
207 concave or convex, but rather it is more often irregularly sigmoidal. We believe that this way of
208 accurately capturing body curvature explains that the variation related to changes in body
209 arching is not observable in principal PCs. The Tps-unbending method also offers additional
210 advantages, for instance, magnifying undetectable Procrustes variance in other landmarks, that is
211 not attribute to geometric distortion.

212

213 To date, no study has used geometric morphometrics to explore the biological factors influencing
214 *rigor mortis*-induced body arching in fossil fishes. Our results indicate a significant correlation
215 between specimen size and curvature, with smaller and more slender individuals exhibiting a
216 more pronounced curvature. This association could be explained by the degree of ossification
217 that seems to be linked to skeletal arching (Pan et al., 2015; Martín-Abad & Poyato-Ariza,
218 2016b). However, our analysis reveals a significant equivalence in body arching between *R.*
219 *gregalis* and *G. conquensis*, suggesting that, in our specific case, taxonomic identity is not linked
220 to the magnitude of body arching. This result counters previous results suggesting that
221 (Bieńkowska-Wasiluk, 2004). It is possible that the morphological and anatomical differences
222 between the species studied here were insufficient to significantly impact the taphonomical
223 processes responsible for generating the curvature or even these biological differences may not
224 be causally related to body arching, as has been seen in experimental studies with extant fishes
225 that refuted any association (Ando et al., 1991). Although curvature is often attributed to
226 taphonomic processes (i.e., *rigor mortis*), there are cases where it holds biological significance.
227 To avoid correcting curvature of natural origin (non-taphonomic), it is essential to select the
228 appropriate landmarks for their use in the straightening protocol. For instance, in our case, the
229 anterior point of the premaxilla and the vertebral column form an axis that marks the straightness
230 of the organism. However, in other cases, this axis may be defined by different landmarks that
231 must be considered after prior anatomical evaluation of the sample.

232

233 Given these considerations, our results represent a step towards correcting the effect of body
234 arching in fossil fishes that can be extended to any particular case study. The more similar the
235 species are (at least based in general shape morphology), the larger the effect of the curvature
236 will have into blurring morphological and biological data, thus reverberating in lowering the
237 resolution of morphometric studies (Clarke & Friedman, 2018; Kammerer et al. 2020; present
238 study), particularly if statistical inference is intended. Namely, correcting this variability is

239 advisable because it can hamper the evaluation of important evolutionary phenomena such as
240 allometry, integration and modularity.

241

242

243 **Conclusions**

244 Two different methods have been designed to correct variation associated with body arching
245 from a landmark configuration, using two well-identified gonorhynchiform fishes from the Las
246 Hoyas fossil site, *Rubiesichthys gregalis* and *Gordichthys conquensis*, as a case sample. A
247 multivariate regression, based on the regression of the Procrustes Data against the assessed
248 degree of arching (Regression-unbending method) corrects such effect. However, details of
249 arching are distributed in the matrix of variance-covariance, and thus might appear in further
250 statistical analyses. Therefore, we recommend using the unbending function of TpsUtil (Tps-
251 unbending method) to get rid of the largest amount of variation related to body arching. We also
252 show that curvature largely depends on the size of the fish (smaller ones tending to be more
253 curved), thus being an important factor to consider in order to ensure accurate and meaningful
254 analyses. No evidence of differences in curvature were related to taxonomic identity, but this
255 needs to be further tested with samples encompassing higher morphological and taxonomical
256 diversity.

257

258 **Acknowledgements**

259

260 The authors express gratitude to the Museo Paleontológico de Castilla-La Mancha for providing
261 access to the Las Hoyas collection. We extend our appreciation to Dr. G. Navalón and Dr. S.M.
262 Nebreda for their valuable discussions, which have enhanced the manuscript, as well as for
263 generously sharing their R code, which was utilized to adapt certain aspects of the R code
264 presented in this work. We want to thank the editors and anonymous reviewers for offering
265 constructive comments which have greatly enhanced the quality and clarity of this manuscript.

266

267

268 **References**

- 269 1. Adams, D. C., & Otárola-Castillo, E. (2013). geomorph: an R package for the collection and
270 analysis of geometric morphometric shape data. *Methods in ecology and evolution*, 4(4), 393-
271 399.
- 272 2. Ando M., Toyohara H., Shimizu Y. & Sakaguchi M (1991). Post-mortem tenderization of fish
273 muscle proceeds independently of resolution of rigor mortis. *Nippon Suisan Gakkaishi*, 57(6),
274 1165-1169
- 275 3. Bieńkowska-Wasiluk, M. (2004). Taphonomy of ichthyofauna from an Oligocene sequence
276 (Tylawa Limestones horizon) of the Outer Carpathians, Poland. *Geological Quarterly*, 48.
- 277 4. Bieńkowska-Wasiluk, M. (2010). Taphonomy of Oligocene teleost fishes from the Outer
278 Carpathians of Poland. *Acta Geologica Polonica*, 60(4), 479-533.

- 279 5. Bookstein, F. L. (1997). Morphometric tools for landmark data: geometry and biology.
280 Cambridge University Press
- 281 6. Cardoso, A. R., Romero, G. R., Osés, G. L., & Nogueira, A. C. R. (2020). Taphonomy of
282 lacustrine fish fossils of the Parnaíba Basin, northeastern Brazil: spatial and causative relations
283 of Konservat Lagerstätten in West Gondwana during Jurassic-Cretaceous. *Palaeogeography,*
284 *Palaeoclimatology, Palaeoecology*, 542, 109602.
- 285 7. Chellouche, P. (2016). *Comparative actinopterygian fish taphonomy of laminated fossil*
286 *Lagerstätten: case studies from the late Mesozoic of Eurasia* (Doctoral dissertation, Friedrich-
287 Alexander-Universität Erlangen-Nürnberg (FAU)).
- 288 8. Chellouche, P., Fürsich, F. T., & Mäuser, M. (2012). Taphonomy of neopterygian fishes from
289 the Upper Kimmeridgian Wattendorf Plattenkalk of Southern Germany. *Palaeobiodiversity*
290 *and Palaeoenvironments*, 92(1), 99-117.
- 291 9. Clarke, J. T., & Friedman, M. (2018). Body-shape diversity in Triassic–Early Cretaceous
292 neopterygian fishes: sustained holostean disparity and predominantly gradual increases in
293 teleost phenotypic variety. *Paleobiology*, 44(3), 402-433.
- 294 10. Dietl, G., & Schweigert, G. (2011). Im Reich der Meerengel–Fossilien aus dem Nusplinger
295 Plattenkalk. *Munich: Pfeil*.
- 296 11. Fruciano, C., Schmidt, D., Ramírez Sanchez, M. M., Morek, W., Avila Valle, Z., Talijančić,
297 I., Pecoraro C. & Schermann Legionnet, A. (2020). Tissue preservation can affect geometric
298 morphometric analyses: a case study using fish body shape. *Zoological Journal of the Linnean*
299 *Society*, 188(1), 148-162.
- 300 12. Haas, T. C., & Orleans, N. (2011). Guide to the “Unbend Specimens” module in tpsUtil. *March*
301 *J. Fish. Biol*, 1-4.
- 302 13. Hellowell, J., & Orr, P. J. (2012). Deciphering taphonomic processes in the Eocene Green
303 River formation of Wyoming. *Palaeobiodiversity and Palaeoenvironments*, 92(3), 353-365.
- 304 14. Kammerer, C. F., Deutsch, M., Lungmus, J. K., & Angielczyk, K. D. (2020). Effects of
305 taphonomic deformation on geometric morphometric analysis of fossils: a study using the
306 dicynodont *Diictodon feliceps* (Therapsida, Anomodontia). *PeerJ*, 8, e9925.
- 307 15. Marramà, G., Bannikov, A. F., Tyler, J. C., Zorzin, R., & Carnevale, G. (2016). Controlled
308 excavations in the Pesciara and Monte Postale sites provide new insights about the
309 palaeoecology and taphonomy of the fish assemblages of the Eocene Bolca Konservat-
310 Lagerstätte, Italy. *Palaeogeography, Palaeoclimatology, Palaeoecology*, 454, 228-245.
- 311 16. Monteiro L.R. 1999. Multivariate regression models and geometric morphometrics: the search
312 for causal factors in the analysis of shape. *Syst. Biol.* 48:192–199.
- 313 17. Navalón, G., Bjarnason, A., Griffiths, E., & Benson, R. B. (2022). Environmental signal in the
314 evolutionary diversification of bird skeletons. *Nature*, 1-6.
- 315 18. Pan, Y., Fürsich, F. T., Chellouche, P., & Hu, L. (2019). Taphonomy of fish concentrations
316 from the Upper Jurassic Solnhofen Plattenkalk of Southern Germany. *Neues Jahrbuch für*
317 *Geologie und Paläontologie-Abhandlungen*, 292(1), 73-92.
- 318 19. Pan, Y., Fürsich, F. T., Zhang, J., Wang, Y., & Zheng, X. (2015). Biostratigraphic analysis of
319 Lycoptera beds from the Early Cretaceous Yixian Formation, western Liaoning,
320 China. *Palaeontology*, 58(3), 537-561.

- 321 20. Poyato-Ariza, F. J. (1996). A revision of *Rubiesichthys gregalis* WENZ 1984 (Ostariophysi,
322 Gonorynchiformes), from the Early Cretaceous of Spain. *Syst. Paleoecol*, 1984, 329-348.
- 323 21. Martín-Abad, H. & Poyato-Ariza, F.J. (2016a). Osteichthyan fishes. En: F.J., Poyato-Ariza y
324 A.D. Buscalioni, (Eds.). *Las Hoyas: A Cretaceous wetland*. (pp. 114-132) München: Verlag
325 Dr. Friedrich Pfeil.
- 326 22. Martín-Abad, H., & Poyato-Ariza, F.J. (2016b). Biostratinomic factors involved in fish
327 preservation. Osteichthyan fishes. En: F.J., Poyato-Ariza y A.D. Buscalioni, (Eds.). *Las*
328 *Hoyas: A Cretaceous wetland*. (pp. 114-132) München: Verlag Dr. Friedrich Pfeil.
- 329 23. R Core Team (2023). R: A Language and Environment for Statistical Computing. R
330 Foundation for Statistical Computing, Vienna, Austria. <<https://www.R-project.org/>>.
- 331 24. Rohlf, F. (2015). The Tps series of software. Hystrix. 26. 1-4. 10.4404/hystrix-26.1-11264.
- 332 25. Roth, B., Slinde, E., & Arildsen, J. (2006). Pre or post mortem muscle activity in Atlantic
333 salmon (*Salmo salar*). The effect on rigor mortis and the physical properties of
334 flesh. *Aquaculture*, 257(1-4), 504-510.
- 335 26. San Román, C., Cambra-Moo, Ó., & Martín-Abad, H. (2023). How to quantify taphonomic
336 alteration? A novel index for fossil fish collections. *Historical Biology*, 1-7.
- 337 27. Schlager, S. (2017). Morpho and Rvcg–Shape Analysis in R: R-Packages for geometric
338 morphometrics, shape analysis and surface manipulations. In *Statistical shape and*
339 *deformation analysis* (pp. 217-256). Academic Press.
- 340 28. Seilacher, A., Reif, W. E., & Westphal, F. (1985). Sedimentological, ecological and temporal
341 patterns of fossil Lagerstätten. *Philosophical Transactions of the Royal Society of London. B,*
342 *Biological Sciences*, 311(1148), 5-24.
- 343 29. Sotola, V. A., Craig, C. A., Pfaff, P. J., Maikoetter, J. D., Martin, N. H., & Bonner, T. H.
344 (2019). Effect of preservation on fish morphology over time: Implications for morphological
345 studies. *PloS one*, 14(3), e0213915.
- 346 30. Valentin, A. E., Penin, X., Chanut, J. P., Sévigny, J. M., & Rohlf, F. J. (2008). Arching effect
347 on fish body shape in geometric morphometric studies. *Journal of Fish Biology*, 73(3), 623-
348 638.
- 349 31. Viohl, G. (2015). Die Plattenkalk-Typen der Südlichen Frankenalb. In G. Arratia, H.-P.
350 Schultze, H. Tischlinger, & G. Viohl (eds.), Solnhofen. Ein Fenster in die Jurazeit (pp. 72–77).
351 München: Pfeil
- 352 32. Weiler, W. (1929). Über das Vorkommen isolierter Köpfe bei fossilen
353 Clupeiden. *Senckenbergiana*, 11(1/2), 40-47
- 354 33. Zelditch, M., Swiderski, D., & Sheets, H. D. (2012). Geometric morphometrics for biologists:
355 a primer. *Academic press*.

Figure 1

Study sample and landmark configuration.

(A) *Rubiesichthys gregalis* MUPA-LH- 545a. (B) *Gordichthys conquensis* MUPA-LH-2179a. (C) Landmark configuration placed on MUPA-LH-1386a. (D) Outline drawing, landmark configuration and index of curvature (IC) measurements of MUPA-LH-1386a. Bar scale= 1 cm. Detailed landmark description are provided in Table 1 of Supplementary File 3. Photo and outline drawing credit: Carla San Román.

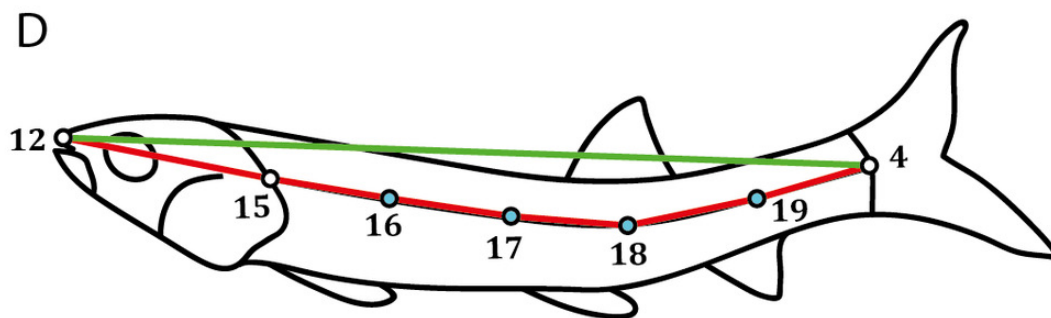
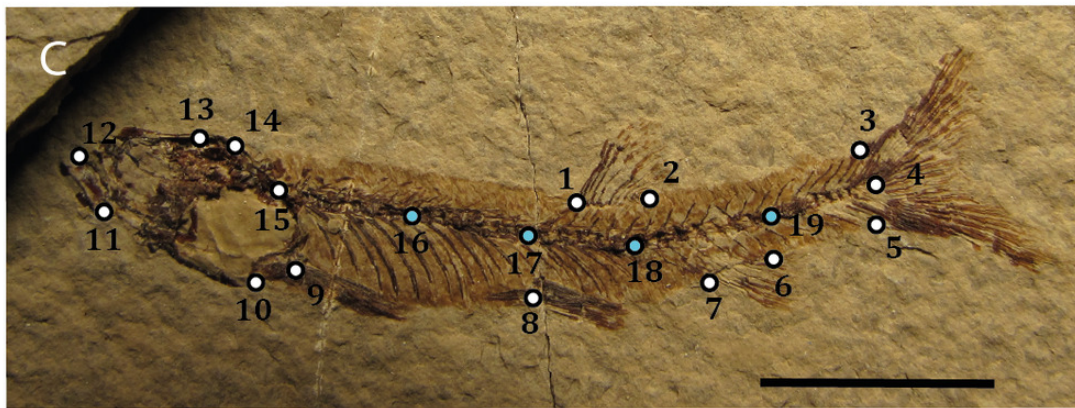


Figure 2

Relation between shape data and index of curvature.

(A) Multivariate regression of shape scores (Procrustes data) to the index of curvature. Shape visualizations are included, where higher values correspond to curved specimens; (B) Regression of the index of curvature to centroid size. *R. gregalis* in purple squares symbols, *G. conquensis* in orange circles symbols. The size of the specimens is represented as the size of the point, following the scale of the legend. Statistical results are provided in Table 3 and Table 5 of Supplementary File 3.

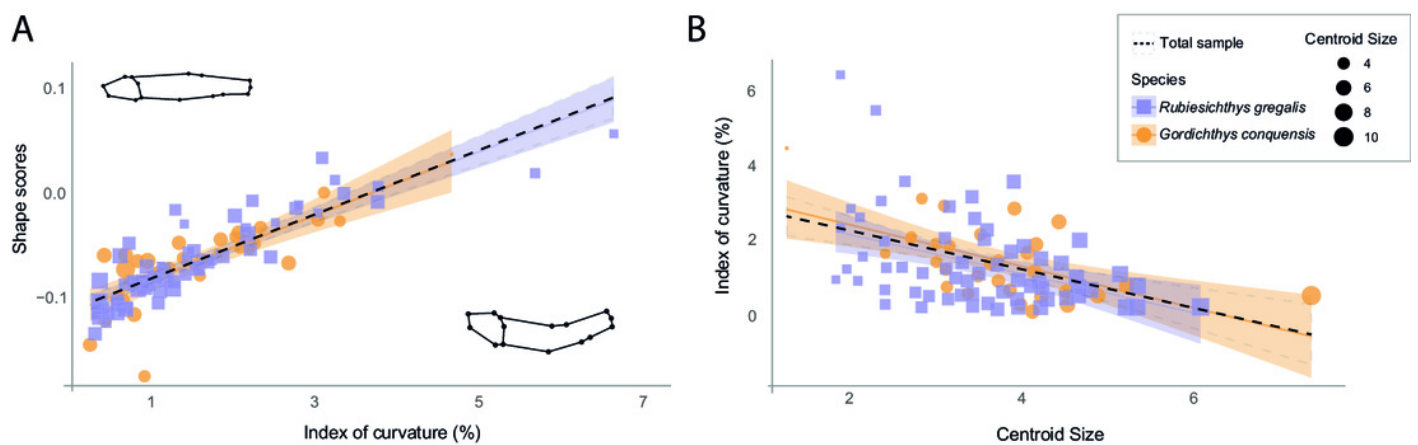


Figure 3

Figure 3. PCA applied to original, Regression-unbending, and TPS-unbending data.

Procrustes variances of the first six principal components (PC) and the subsequent shape variation corresponding to each PC for the original and modified (Regression-unbending and Tps-unbending) data.

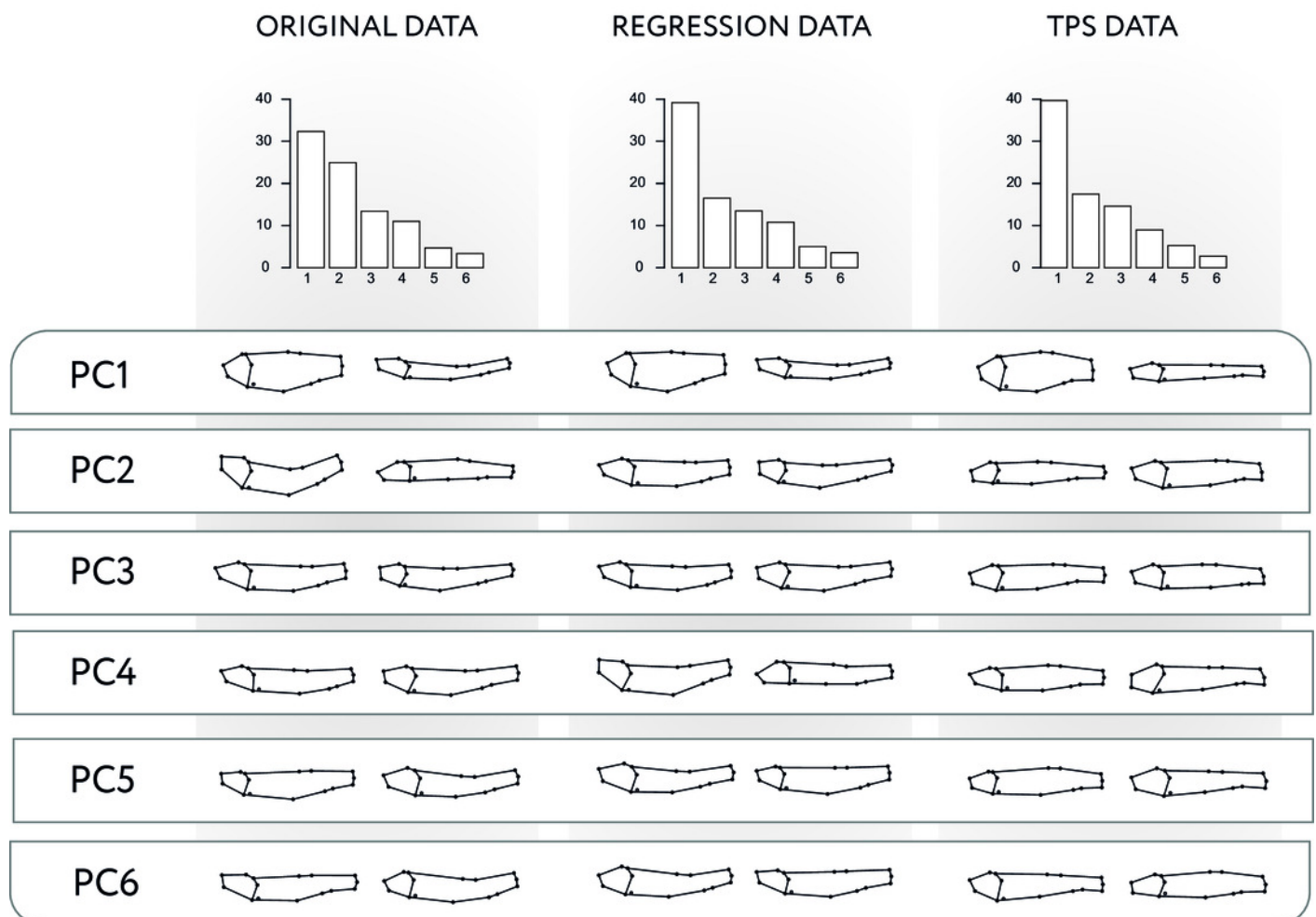


Figure 4

Procrustes variance per landmark.

The gradient from gray to red indicates, respectively, the minimum and maximum Procrustes variance: (A) in each data; (B) in aggregate for all samples. The mean values of Procrustes variance per landmark are provided in the Table 9 of Supplementary File 3.

